

Physics and Physiology of Ventilation-Perfusion Coupling: Substantiation and Initial Experience of End-Expiratory Pressure Choice During Mechanical Ventilation

© R.Yu. Ovsianikov,¹ T.A. Gromova,¹ V.A. Moloshneva,² A.N. Kovalenko,^{2,3} K.M. Lebedinskii^{1,4}

¹ Mechnikov North-Western State Medical University, St. Petersburg, Russia

² ITMO University, St. Petersburg, Russia

³ Ioffe Institute, St. Petersburg, Russia

⁴ Federal Research and Clinical Center of Intensive Care Medicine and Rehabilitation, Moscow, Russia

e-mail: mail@lebedinski.com

Received February 8, 2022

Revised February 4, 2022

Accepted April 4, 2022

Alveolar gas flow competition with pulmonary capillary blood flow for restricted space within lungs during mechanical ventilation, which is well known in respiratory physiology but neglected in everyday clinical practice, is thoroughly discussed in the paper. Anatomical and physiological conditions of oxygen and carbon dioxide counter-diffusion through alveolar-capillary barrier and the role of ventilation-perfusion relationship are described, and the possibility of blood flow displacement from opened alveoli with high pressure inside to poorly ventilated compartments of low intra-alveolar pressures is demonstrated. Commercially available metabolographic and real-time gas analysis monitors from different manufacturers were used for optimal PEEP adjustment by means of pulmonary $\dot{V}O_2$ and $\dot{V}CO_2$ shifts comparison, influence of patient volaemic status on the physiologic possibility of alveolar recruitment is discussed. Limitations of modern approach to the mechanical lung ventilation aimed at maximal lung opening in underlined and refuted with consideration on effective diffusion surface changes. Inefficacy of mechanical ventilation is especially obvious when acute respiratory failure follows ventilation-perfusion mismatch, like it appears in COVID-19. Partially it can explain discouraging mechanical ventilation outcomes during current pandemic

Keywords: ventilation-perfusion relationship, mechanical ventilation, end-expiratory pressure, indirect calorimetry, metabolograph.

DOI: 10.21883/TP.2022.07.54481.27-22

Introduction

Artificial mechanical lung ventilation (MV) by insufflation method is one of the most efficient, but at the same time most aggressive replacement method for life-supporting bodily functions in case of acute or chronic respiratory failure. For the recent two decades, one of the most important MV objective has been the maximum lung recruitment, i.e. involvement in the ventilation of all alveoli which may be opened (Open up the lung and keep it open!) [1,2]. However, one fact is ignored, i.e. alveolar recruitment and maintenance in open state is only possible in some clinical situations at such intra-alveolar pressure when perfusion of pulmonary capillaries surrounding these alveoli is avoided causing reduction of diffusing lung capacity and many cases — pulmonary blood flow redistribution to unventilated lung fields with hypoxemia aggravation. This phenomenon known in the respiratory physiology from at least classic papers by J.B. West in the early 1960s [3] does not attract much attention of clinical physicians and is not used for MV setting primarily due to the fact that no pulmonary gas effective diffusion surface variation assessment method suitable for everyday clinical use has been available till now.

This paper is devoted to physical and physiological bases of such method, method description and implementation tools.

1. Physical and anatomico-physiological conditions of pulmonary gas diffusion

In term of physics, human and animal lungs are an inert two-phase mass exchanger, where oxygen O_2 diffuses from gas to liquid phase and carbon dioxide CO_2 diffuses in the opposite direction from a single diaphragm. Gas phase is represented by alveolar gas which is exchanged by means of reciprocating convection through a tracheobronchial tree (ventilation V , $l \cdot \text{min}^{-1}$), liquid phase is represented by blood in pulmonary capillaries which entangle the alveoli, this blood flows from the pulmonary artery into the pulmonary veins (perfusion Q , $l \cdot \text{min}^{-1}$), and the diffusion diaphragm is represented by a blood-air barrier, as physiologists call it, including alveolar epithelium, pulmonary capillary endothelium and their basal membranes [4]. The total alveoli internal surface area of an adult is equal to 80–120 m^2 , and the average contact time of each

erythrocyte with alveolar gas (in three alveoli on average) is about 750 ms [5].

And carbon dioxide whose dipole molecule is well soluble in biological fluids and cell membranes diffuses at minimum transmembrane partial pressure gradients while poorly soluble oxygen requires a much higher partial pressure gradient to ensure the diffusion flow which usually is numerically higher than CO₂ flow. Thus, in physiological conditions, oxygen partial pressure in venous admixture $P\bar{v}O_2$ is on average equal to 35–45 mm Hg, in alveolar gas PAO_2 it is 100–110 mm Hg, in arterial blood PaO_2 it is approximately 90–100 mm Hg. At the same time, partial pressure of carbon dioxide in venous admixture $P\bar{v}CO_2$ is on average 46–52 mm Hg, and in alveolar gas $PACO_2$ and arterial blood PaO_2 it is approximately equal 36–42 mm Hg. Thus, alveolo-arterial differential pressure for oxygen $A-aDO_2$ is normally equal to 7–10 mm Hg, while for carbon dioxide $A-aDCO_2$ it is close to zero [4,6].

According to the first diffusion law formulated in 1855 by Adolf Eugen Fick (1829–1901), diffusion flow J with amount of substance per unit time is in general defined as follows:

$$J = -D \frac{d\varphi}{dx}, \quad (1)$$

where minus sign denotes diffusant movement towards concentration decrease, D is the diffusion coefficient in units of area to time ratio, φ is the substance concentration in units of amount of substance to volume ratio, x is the linear coordinate in units of length [7].

To ensure gas exchange through the diaphragm, volumetric diffusion rate V_x will be defined by the diaphragm properties (diaphragm diffusion coefficient D_x for substance X depending on the substance-related permeability of the diaphragm, area S and thickness d) as well as transmembrane partial gas pressure (stress) difference ΔP [6,8]:

$$V_x = D_x \frac{S}{d} \Delta P. \quad (2)$$

No matter how unexpected this could be at first sight, diaphragm area and partially diaphragm thickness are the most variable parameters: effective contact surface between alveolar gas and pulmonary capillary blood may be changed by respiratory phases that change the alveolar diameter and by the right ventricular pulse wave through the pliable pulmonary capillary bed and the diffusion barrier thickness depends on the degree of mechanical tension and extravascular water volume in the pulmonary tissue [4,8,9].

To understand further discussion, let's remember the main features of structural and functional arrangement of lungs. Physiologists define two functional zones — conductive zone where mass transfer is performed by convection and diffusion zone [9]; the boundary between them is functional rather than anatomic and shifts towards the alveolar lumen at high ventilation rates [10,11]. In terms of anatomy, the first zone corresponds to airways

(anatomical dead space whose volume is $2.2 \text{ ml} \cdot \text{kg}^{-1}$ of body weight [6]), the second zone corresponds to alveoli. Airways provide 23 branching generations with gradual increase in the total cross-section from tracheae and main bronchi to bronchiole and alveolar saccules [8]; diffusion process is assumed to be possible beginning from the 16th branching generation (while gas diffusion itself not related to external respiration, e.g. ethanol vapor release and absorption, is possible throughout all airways supplied with bronchial arterial blood [12]). Venous admixture in its turn flows to the lungs from the right heart chambers via pulmonary arteries which branch similar to bronchi and finally form pulmonary capillaries which entangle the alveoli. Oxygenated and carbon dioxide-free arterial blood is accumulated further in the pulmonary veins ending into the left atrium.

If we assume that the alveoli shape may be approximated by spheres of various diameter (in adults, inspiratory alveoli diameter is 0.3–0.5 mm, expiratory alveoli diameter is 0.1–0.2 mm), and the pulmonary capillary shape is approximated by ellipsoidal cross-section tubes with various centerlines (their size does not exceed $10 \mu\text{m}$) [5,6,8,9], impossible close-packed arrangement of such anatomic structures without generation of significant free space between them becomes geometrically evident. In morphology, this space is known as pulmonary interstitium, moreover, points of tight contact between alveoli and pulmonary capillaries where alveolar capillary epithelium and endothelium have common basal diaphragm are known as „thin zone“ (here minimum diffusion diaphragm thickness is $\leq 0.7 \mu\text{m}$ [6]), and the remaining space beyond gas- and blood-carrying lumen is known as „thick zone“ of the pulmonary interstitium. It should be noted that such spatial structure composed of interconnected spheres and polygons which may be represented by honeycomb used as visual flat equivalent considerably restricts the simultaneous cell size increase range without breaking the connecting links. This is the factor which is behind the shear stress damaging mechanism [13,14] causing rupture of primarily pulmonary vessels and gas ingress into the pulmonary interstitium during excessive alveoli inflation in the MV process.

It is evident from the above that lung tissue is mechanically heterogeneous — it includes a relatively rigid „skeleton“ represented by bronchi whose walls are reinforced with cartilaginous rings with a diameter up to approximately 1.5–2 mm [6], and with large vessels, and pliable alveolar „foam“ strung on the skeleton. This parenchyma is limited on the outside by dense pulmonary pleurae, including interlobar pleura which splits the lung tissue in various planes. This lung tissue heterogeneity allows separate „compartments“ to form in pathological conditions with pressure other than that of the surrounding lung tissue. In its turn, bronchi or vessel lumen blocking by mucus, exudate, thrombi or mechanical kinking causes the situation when pressure transfer inside these cavitory systems is not possible and Pascal's law in lungs is not fulfilled.

Understanding of these facts is essential for our further discussion.

2. Ventilation/perfusion ratios and stabilization physiology

Anatomical possibility of blood and gas flows engagement certainly depends on the variety of physiological or pathological conditions. The simplest „student“ model of ventilation-perfusion imbalance was shown by R. Riley and A. Cournand [15] in 1949 (Figure 1). It suggests that, in addition to „ideal“ alveoli AL whose ventilation V_A is combined with perfusion P of capillaries C (in center), lungs also have unventilated alveoli whose capillaries are still perfused, and, thus, they pass venous admixture V bypassing the pulmonary gas exchange directly into the left heart chambers. In addition, a totally opposite „breakage“ is also demonstrated — alveoli in which ventilation is present, but capillary perfusion is absent and which produce a so called alveolar (or physiological) „idle ventilation“ dead space. All these three radical scenarios shown in Figure 1 actually exist in any lung. However, the stochastic nature of ventilation and perfusion distribution processes in hundred million (!) alveoli and capillaries of each lung ascertain that the entire ventilation/perfusion ratio range is represented even in a normal organ — from very high to infinitely small values [5], and a qualitative difference between normal and illness conditions defines their different statistical distributions whose peak in the first case shall fall within an optimum value range.

Actually, in 1946, American physiologists H. Rahn and W Fenn demonstrated alveolar gas composition vs. local ventilation/perfusion ratio curves [16]. This nomographic chart (Figure 2) shows that the best pulmonary gas exchange function is achieved at a rather fixed ventilation/perfusion ratio (V/Q) which is approx. 0.8. It can be seen that curve PAO_2 in the vicinity of this abscissa value has a rather steep run reflecting quick hypoxia development at growing excessive perfusion. Precisely this excessive perfusion mechanism in unthrombosed pulmonary vascular

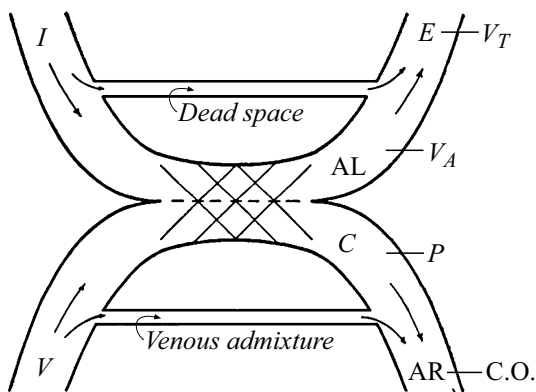


Figure 1. Diagram of alveolar dead space formation and venoarterial bypass in lungs (from [15], 1949).

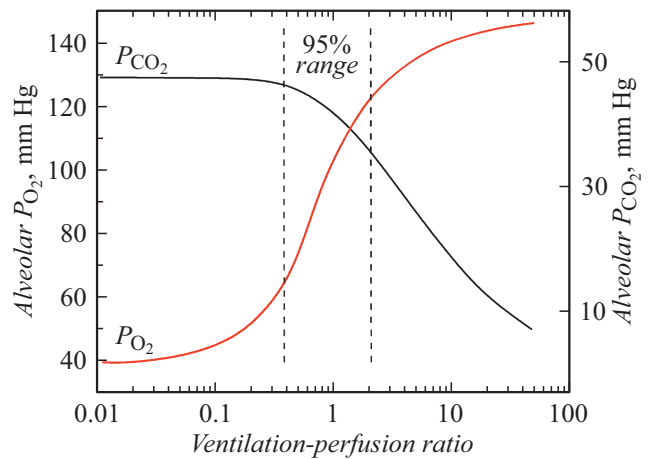


Figure 2. Nomographic chart of the alveolar gas composition depending on the ventilation/perfusion ratio (from [16], 1946): x-axis — is V/Q , left y-axis — PAO_2 , mm Hg, these values are represented by a red ascending curve designated as P_{O_2} , right y-axis — $PACO_2$, mm Hg, these values are represented by a black descending curve designated as P_{CO_2} .

areas which are visible on an X-ray computer tomography image as „ground glass opacities“ [17] explains the deep hypoxemia development in COVID-19 novel coronavirus infection (nCoV) patients whose pulmonary capillaries are affected by microvascular obliterating thrombovasculitis (MicroCLOTS, [18]). The importance of maintaining optimum V/Q is also emphasized by many mechanisms (see the Table below) due to which ventilation and blood flow conditions are unstable in acini with non-optimum V/Q [5].

Primarily, ventilation/perfusion imbalances are prevented by ambidextrous physiological mechanisms known as Ulf S. von Euler — Göran Liljestrand (1946) [19] and John W. Severinghaus — Edward W. Swenson (1961) [20] phenomena. Being implemented by means of pulmonary vessel and bronchi smooth muscle contraction as a result of local metabolic processes without involvement of any nervous system division, these mechanisms prevent formation of an intrapulmonary bypass and alveolar dead space and, thus, cause the spasm of pulmonary artery branches which perfuse poorly-ventilated lung regions and, ambidextrally, spasm of bronchioles through which lung tissue areas with low blood flow are ventilated. intrapulmonary bypass formation due to excessive perfusion is also prevented by F.Ya. Kitaev’s reflex (1931) resulting in pulmonary arteriolar spasm during an increase in the left atrium and pulmonary vein pressure [5]. An important role in proper correlation of ventilation and perfusion variations is played by mechanical coupling of contractile components of pulmonary vessel and bronchiole walls when a smooth muscle cell get round the adjacent bronchiole and vessel in a figure of „eight“ [6], as well as a codirectional effect of most biologically active substances on bronchi and

Optimum ventilation/perfusion ratio maintenance mechanisms

<p>Von Euler–Liljestrand mechanism (1946): reduced ventilation → vasoconstriction</p> <p>Severinghaus–Swenson phenomenon (1961): reduced perfusion → bronchospasm</p> <p>Kitaev’s reflex (1931): pressure growth in pulmonary veins and left atrium → pulmonary arteriola spasm</p> <p>Mechanical coupling of vessel and bronchiole walls</p> <p>unidirectional action of most of substances on smooth muscles of bronchi and vessels</p> <p>Collateral ventilation:</p> <ul style="list-style-type: none"> • pores of Kohn (alveola ↔ alveola) • channels of Martin (bronchiole ↔ bronchiole) • canals of Lambert (bronchiole ↔ alveola) <p>Collateral blood flow within a capillary net</p> <p>Blood flow influence on surfactant production</p> <p>Gravity (J.West): blood flow is better at the bottom where the ventilation is better</p>

pulmonary vessels: bronchoconstrictors are predominantly vasoconstrictors and bronchodilators are vasodilators [5,21].

Collateral ventilation mechanisms —are morphologists’ discovery that led physiologists to revise their opinions: it had been believed for a long time that full bronchus or bronchiole obstruction at any branching level necessarily causes atelectasis — collapse of a corresponding lung region as a result of full alveolar gas absorption by blood [6]. Meanwhile, anatomical „horizontal“ interactions between adjacent bronchioles (channels of Martin), alveola and adjacent bronchiole (canals of Lambert) and adjacent bronchiole alveoli (pores of Kohn) not only explained how patients can expectorate bronchial casts, but also led to revise the concept of bronchoalveolar „tree“ structure where each leaf has only one way of communication with roots in favor of „sponge“ where alveoli randomly interact vertically and horizontally [9]. Pulmonary vascular bed branching also follows a fractal pattern only to the small arteria level while the capillary net abundant in „horizontal“ interactions does not follow the scalable self-similarity symmetry any longer [5]. Collateral alveoli ventilation and capillary blood flow route variability mechanisms significantly prevent V/Q imbalance in case of bronchiole and small vessel obstruction.

An important role in alveoli stability maintenance is played by a surface-active agent (surfactant) — dipalmitoylphosphatidylcholine synthesized by so called type II alveolocytes which covers the surface of all alveolar epithelium cells facing the lumen. Thanks to this lipid film which reduces surface tension, spontaneous alveoli collapse trend is compensated to a large extent [6,9]. However, the energy-consuming surfactant synthesis and secretion process requires not only oxygen (absorbed from the alveoli lumen in this case), but also biological oxidation substrates and applicable plastic material which are supplied with blood flow. Therefore, the pulmonary perfusion restriction naturally causes surfactant synthesis reduction which in its

turn causes alveoli collapse by limiting the alveolar dead space formation.

Finally, the gravity factor plays an important role in the physiological blood flow distribution. In homo erectus and great apes, vertical dimension of lungs may exceed 30 cm, and this creates ultimately uneven conditions for blood and alveolar gas flows due to the difference in their density because both lung fluids in physiological conditions are continuous and Pascal’s Law is fulfilled for them. In the 1960s, J.B. West in the west [3] and A.P Zilber in the USSR [22] managed to show that, already in physiological conditions, actual pressure ratio allows alveolar gas to compete with pulmonary capillary blood for the internal lung volume which hinders the lung apex perfusion in vertical body position and in general creates

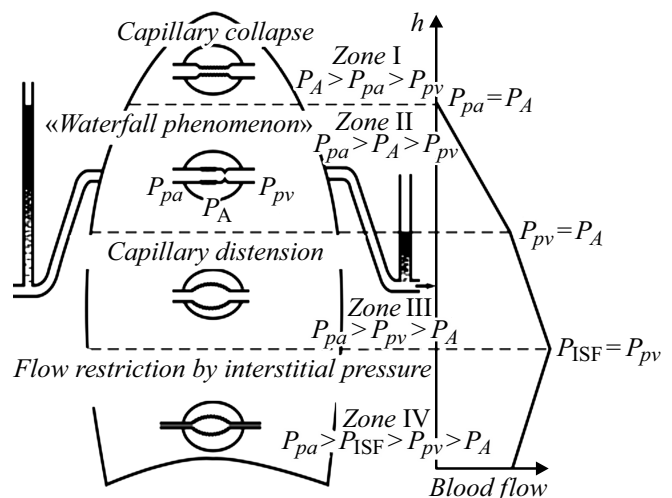


Figure 3. J. West’s zones (from [23]). P_A — pressure in alveoli, P_{pa} — pressure in the arterial elbow of pulmonary capillaries, P_{pv} — pressure in the venous elbow of pulmonary capillaries, P_{ISF} — liquid pressure in pulmonary interstitium.

a natural gradient of ventilation/perfusion ratios in vertical lung dimension (Figure 3).

Lungs are divided into four typical zones with different ventilation/perfusion ratios, they are called J West's zones (1963). In the first highest zone, intra-alveolar pressure P_A exceeds that in the arterial part of pulmonary capillaries P_{pa} , and due to this alveoli completely mechanically constrict the capillary blood flow. In the second zone, P_A is lower than P_{pa} , it exceeds the venous end pressure in pulmonary capillaries P_{pv} causing a wavy, intermittent behavior of pulmonary capillary blood flow („waterfall phenomenon“) determined by the respiratory cycle phases. In the third „Capillary distension“ zone, perfusion becomes continuous because $P_{pa} > P_{pv} > P_A$ [3]. Finally, in the lowest fourth zone described later by J.M.B. Hughes (1968), capillary blood flow restriction by hydrostatic pressure in the pulmonary interstitium P_{ISF} [23] shall be taken into account. Eventually, as can be noted, maximum perfusion is displaced into the lower lung fields under gravity where more intensive intra-alveolar gas volume exchange corresponds to it. Thus, the local pulmonary perfusion irregularity, in particular, its vertical gradient, is another V/Q ratio optimization factor, but conditions for capillary blood flow displacement by gas pressure in alveoli lumen (zone I) may occur even at low intra-alveolar pressures inherent in unassisted breathing ($\pm 2-3$ mbar).

3. MV biomechanics

During unassisted physiological inspiration, air flows into the lungs with contraction of diaphragm which creates depression in pleural cavities compared with atmospheric pressure; alveolar pressure fluctuations are equal to $\pm 2-3$ mbar [8]. By contrast, MV performed by a common air insufflation method involves creation of positive alveolar pressure which fluctuates depending on respiratory phase usually within 5–20 mbar, but may reach 40 mbar in some situations [24]. Thus, in MV conditions, compared with unassisted breathing, not only high and low pressure phase inversion, but also significant growth of pressure fluctuation amplitude and absolute pressure values take place.

„Ventilator–patient“ system action in MV conditions is generally analyzed using a rather simple model (Figure 4, a), where the ventilator circuit and patient's respiratory ways are together represented by a tube with air-flow resistance R , and the „chest–lungs“ system (consisting of the expanded lungs and compressed rib cage coupled together by depression in pleural cavities) is represented by an elastic reservoir with elasticity C having a non-zero wall weight [25]. When respiratory gas is injected into the lungs under positive pressure (common insufflation mechanical ventilation), the equation of full pressure measured by the ventilator pressure gauge will be written as

$$P = P_{\text{EEXP}} + \frac{V}{C} + R \frac{dV}{dt} + I \frac{d^2V}{dt^2}, \quad (3)$$

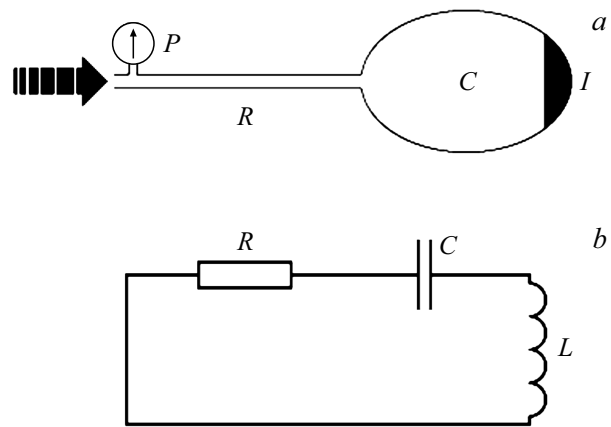


Figure 4. Physical analogy between respiratory system (a) and electrical oscillation circuit (b): P — full pressure measured by the ventilator pressure gauge, R — total air-flow resistance of the circuit and respiratory ways (a) and ohmic resistance of the circuit (b), C — static compliance of lungs and chest (a) and capacitance (b), I — respiratory system inertia, L — coil inductance.

where P_{EEXP} — is the pressure at the end of the previous respiratory cycle (in clinical practice denoted as PEEP — positive end-expiratory pressure), V — is the respiratory gas volume injected into respiratory ways, C — static elasticity of lungs and chest (in practice referred to as static compliance) expressed in $\text{ml} \cdot \text{mbar}^{-1}$, R — is the total air-flow resistance of respiratory ways (in practice referred to as the resistance) expressed in $\text{mbar} \cdot \text{min} \cdot \text{l}^{-1}$, I — is a so called inertia expressed in $\text{mbar} \cdot \text{min}^{-2} \cdot \text{l}^{-1}$. Thus, $1/C$ — is the volume factor, R — is the flow factor, I — is the flow acceleration factor.

Since modern mechanical ventilators are supplied with medical gases from 4–5 at. systems and/or small-frame flow turbine generators, they have no separator (positive displacement chamber) and volume calculation is based on the integration of flow signal $F = dV/dt$ controlled by proportional solenoid valves, equation (3) for the mechanical ventilator control system is as follows

$$P = P_{\text{EEXP}} + \frac{1}{C} \int F(t) dt + RF + I \frac{dF}{dt} \\ \approx P_{\text{EEXP}} + \frac{1}{C} \int F(t) dt + RF, \quad (4)$$

where the fourth term is generally ignored due to its smallness (though behavior I could have characterized, in particular, lung tissue weight variations, for example, during edema).

As can be seen, the system described by equations (3) and (4) has all oscillatory properties, in particular, time constant $\tau = RC$ and natural oscillation frequency $\nu = \sqrt{1/CI}$, and may be described by an analog model in the form of an oscillatory circuit (Figure 4, b) [26]. In MV conditions, the inspiration phase represents forced system fluctuation and the expiration phase represents free fluctuation.

Figure 5 shows pressures P and flows F behavior in the ventilator circuit in volume control ventilation mode (VCV): physician sets the desired inspiration volume V_T , but this is actually flow control according to $V_T = \int_0^{t_i} F(t)dt$ [27]. It should be noted that only one of these variables can be physically controlled at a time — flow or pressure, while the other variable is defined using equation (4) by „ventilator–patient“interaction. Upper physical limits of these variables are interconnected and restricted by the effective mechanical output N delivered by the ventilator into the breathing circuit (since $N = F \cdot P$), and control accuracy is limited by flow and pressure sensors and sensor sampling rate.

The curves in Figure 5 show that the ventilator-assisted inspiration is accompanied with an increase in pressure and volume injected into the lungs according to equation (3). When pressure peak (PPeak) is achieved, the inspiratory valve is closed, but the expiratory valve still remains closed too; finally, due to the fact that flow is reset to zero at permanent V_T , pressure decreases to the inspiratory plateau level:

$$P_{\text{Plateau}} = P_{\text{EEXP}} + \frac{V_T}{C}. \tag{5}$$

Passive expiration which starts after the inspiratory pause t_{IP} is characterized by further circuit pressure decrease and stereotypical expiratory flow dynamics — very quick peak achievement followed by exponential reduction of the volume flow rate. Current alveolar pressure may be estimated using these curves only at zero flow rate and stable pressure, i.e. with stabilized P_{Plateau} and P_{EEXP} during inspiratory pause t_{IP} and expiratory pause t_{EP} , respectively. It is important that alveolar pressure in air-tight breathing circuit does not decrease below P_{EEXP} throughout the respiratory cycle, and in case of improper MV settings (the next inspiration starts at non-zero inspiratory flow!), minimum

alveolar pressure exceeds P_{EEXP} (so called intrinsic PEEP uncontrolled by ventilator pressure gage) [24].

In terms of capillary phenomena, collapsed alveoli recruitment and maintenance in open (spherical) condition require intraluminal pressure which is defined by P.-S. Laplace’s Law (1805):

$$P = \frac{2\sigma}{r}, \tag{6}$$

where σ — is the interfacial surface tension, r — is the alveolus radius (in the range from 0.1 to 0.25 mm, which is by many orders greater than the molecule sizes — Laplace law application condition) [28].

Thus, the required intraluminal alveolar pressure is higher when damage of the surfactant film on the alveolar internal surface is greater and the alveoli diameter is lower.

4. Ventilation/perfusion ratios in Mechanical ventilation conditions

In pathological conditions, more or less long alveolar collapse areas (atelectasis) without lumen may occur and, thus, the pressure from respiratory airways is not transmitted there. Cellular lung tissue structure penetrated by vessels, bronchi and interlobar pleurae forms separate „compartments“ whose pressure differs from that in the surrounding alveoli lumen and the confining walls (e.g. visceral pleura of the right middle lobe) are under transmural pressure. In certain conditions, this may cause rather dramatic pulmonary blood flow redistribution with major ventilation/perfusion imbalances.

The case with patient L. aged 75 who was observed by us in May 2011 [29]. She had massive community-acquired pneumonia with almost total left lung damage affected by severe carbohydrate metabolism disorder (diabetic ketoacidosis) and thoracic spine scoliosis (Figure 6, a) that required mechanical ventilation by insufflation method. The ventilation was carried out with respiratory cycle rate 12 min^{-1} , pressure during assisted inspiratory phase (peak inspiratory pressure - PIP) was constant and equal to 20 mbar above P_{EEXP} level, PEEP 10 mbar was set at the end of expiratory phase, inspiratory time/expiratory time ratio $t_I/t_E = 2 : 1$. And despite the pure oxygen ventilation, severe hypoxemia was observed — PaO_2 was equal to 52.1 mm Hg (with approx. 100 mm Hg specified for atmospheric air breathing).

A natural question occurred — how could the gas exchange function have been hardly survivable in intensive care conditions with virtually intact (and larger by volume!) left lung. The only response observed at that time was pulmonary capillary blood flow displacement from the intact right lung (in whose alveoli the ventilator maintained rather high pressure levels!) into the damaged left lung where no pressure was transmitted and, therefore, free blood flow conditions were created — though without efficient gas exchange capability. In other words, the whole left lung became West’s zone I, where the capillary blood flow was

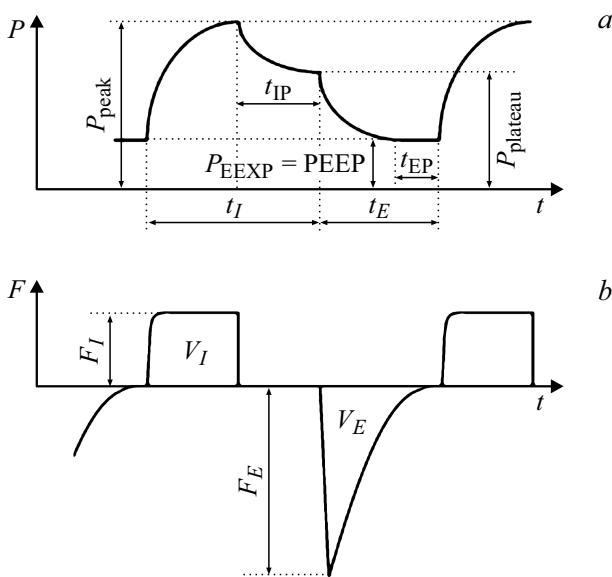


Figure 5. Pressure (a) and flow (b) curves for volume controlled ventilation (VCV) with inspiratory and expiratory pauses.

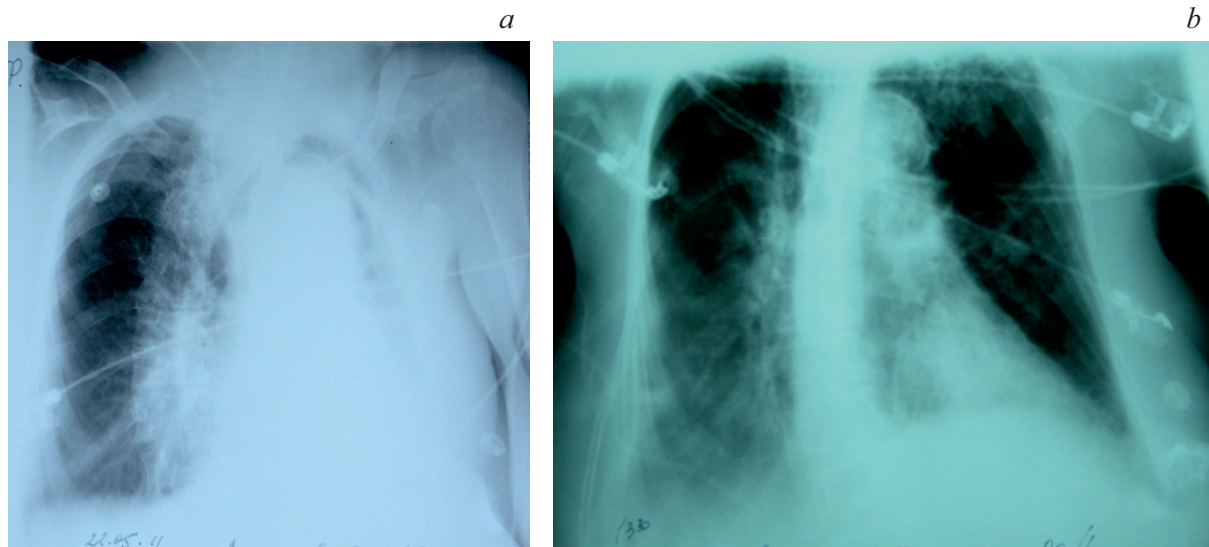


Figure 6. *a* — initial chest X-ray image of patient L; *b* — chest X-ray image of the same patient during differential lung ventilation.

constricted by alveoli inflated by high pressure. When the more pliable right lung assumed the whole mechanical ventilation volume, the same factor caused failure to open the left lung damaged by pneumonia and, thus, more rigid.

A decision was made to perform differential ventilation of the left and right lungs in order to avoid blood flow displacement from the right lung into the left one and to expand the left lung more efficiently as far as possible. For this, the patient was reintubated using Gebauer 35F left-type double lumen endotracheal tube, and a separate mechanical ventilator was connected to each lumen. Respirolix Esprit (USA) ventilator was connected to the left lumen with rate 10 min^{-1} , PIP 20 mbar, PEEP 10 mbar and $t_I/t_E = 2 : 1$; Puritan-Bennet 740 (USA) ventilator was connected to the right lung with rate 14 min^{-1} , inspiratory volume 300 ml, PEEP 10 mbar and $t_I/t_E = 1 : 2$. Different respiratory cycle rates were selected due to our efforts to avoid possibly simultaneous blood flow „constriction“ in both lungs. 30 min after the commencement of differential MV, PaO_2 was 225.2 mbar; inspired oxygen fraction was reduced to 75% in response, and significant increase in the airness of the damaged left lung was also observed after 4 h (Figure 6, *b*). And though the patient died due to pneumonia-induced sepsis progression affected by diabetes, the differential lung ventilation ensured normalized blood gas composition until the last days of her life!

Analysis of this clinical observation got us thinking: if in this case, when the left lung was totally damaged and the right one was virtually intact, the differential ventilation solved the problem of blood flow „squeezing“ into the damaged lung tissue fields — can exactly the same situation occur during uneven damage of the entire lung parenchyma, when the „varied“ X-ray pattern on both sides is indicative of accidental alteration of normal ventilated and damage collapsed areas?

In the most typical case, such pattern occurs in acute respiratory distress syndrome when nonspecific (inflammatory in its pathophysiological nature!) response of the pulmonary parenchyma to the action of various damaging factors causes subdivision of the whole alveoli pool into three „subsets“ — D (Dead, i.e. fatally consolidated and not involved in ventilation any longer), H (Healthy, i.e. relatively undamaged) and R (Recrutable, capable of being involved again into ventilation by adequate pressure application). Understanding of this subdivision led Dutch researcher B. Lachmann to so called „open lung concept“ (1992), the essence of which is expressed by the commonly accepted slogan „Open up the lung and keep it open!“. In this case recruitment is achieved by application of adequate positive inspiratory pressure, while to keep alveoli open, high positive pressure at the end of expiration is required P_{EEEP} (Positive End-Expiratory Pressure - PEEP) [1,26].

Let's discuss how pressures required for these MV treatment conditions correlate with pressures in the pulmonary vascular bed. For example, „ 40×40 “ alveoli recruitment maneuver implies alveoli pressurization at 40 s up to 40 mbar [24], it is not recommended to select PEEP value higher than 24 mbar, and inspiratory pressure level higher than 35 mbar [30]. In this case, the specified upper limit (!) of the average pulmonary artery pressure is not higher than 20 mm Hg, which is only 27 mbar, and normal pulmonary capillary pressures directly measured by the Swan-Ganz catheter in West's zones III–IV are even lower — 8–16 mbar [31]. It is quite clear that in such conditions perfusion displacement from all ventilated lung tissue compartments into damaged (collapsed) compartments with lower pressure is a quite real situation. Only in this case, as opposed to the above clinical observation, differential ventilation of this two alveoli sets dissipated throughout the lung is not practical. . .

Where is the way out? Before COVID-19 pandemic, we already clearly understood that MV taking over, fully or partially, mechanical breathing action which is unbearable for the patient is, in the same time, incapable of solving the ventilation-perfusion imbalance issue — it is not intended for this. But how can we avoid at least direct harm inflicted by mechanical positive-pressure ventilation to correct pulmonary perfusion distribution?

5. Metabolographic monitoring and its capabilities

It appeared that solution can be found by means of analysis of oxygen absorption dynamics and carbon dioxide elimination by lungs which enables to clearly see the moment when recruitment of additional perfused alveoli with an increase in intra-alveolar pressure gives place to blood flow „displacement“ by alveoli, i.e. to West’s zone I expansion. As is evident from the foregoing, in some cases this is accompanied by an increase in intrapulmonary venoarterial blood bypassing — if the lung has corresponding unventilated regions with open (i.e. unthrombosed) capillary bed. Instrument that enabled ventilation/perfusion relationship monitoring in clinical conditions is metabolimeter — the instrument initially designed for aerobic energy metabolism measurement by indirect calorimetry, which, in its turn, enables to reasonably control nutrition of critically ill patients [32].

Calculation of minute carbon dioxide elimination by lungs VCO_2 and minute oxygen absorption in lungs VO_2 implies addition of corresponding elimination and absorption values in each respiratory cycle within a minute. The latter, in turn, are calculated as difference of products of momentary respiratory gas flow F and CO_2 and O_2 concentrations integrated separately during inspiratory phase t_I and expiratory phase t_E :

$$VCO_2 = \sum_0^f \left(\int_0^{t_E} F(t)C_{CO_2}(t)dt - \int_0^{t_I} F(t)C_{CO_2}(t)dt \right), \tag{7}$$

$$VO_2 = \sum_0^f \left(\int_0^{t_I} F(t)C_{O_2}(t)dt - \int_0^{t_E} F(t)C_{O_2}(t)dt \right), \tag{8}$$

where f — is respiratory cycle rate, min^{-1} ; C_{CO_2} — is carbon dioxide volume concentration; C_{O_2} — is volume oxygen concentration. Such calculation requires not only high precision low and concentration measurement, but also flawless synchronization of time series of momentary C_{CO_2} , C_{O_2} and F . In modern commercial medical equipment, carbon dioxide concentration is usually measured by infrared absorption sensors in 4200–4300 nm spectral band, oxygen concentrations are measured by low-lag paramagnetic sensors and gas flows are measured by differential pressure flowmeters or hot-wire anemometers [33,34].

When VO_2 and VCO_2 have been acquired, the instrument calculates respiratory coefficient $RQ = VCO_2/VO_2$, and then uses it to calculate a so called caloric equivalent for oxygen — an indicator which numerically reflects energy effect of consumption of O_2 volume unit in biological oxidation reactions in aerobic approach (i.e. in the absence of lack of oxygen delivery to cells). As could be expected, this effect differs according to the type of substrate to be oxidized (fat, carbohydrate, protein) that enables to determine RQ . Thus, the target variable of the metabolographic monitoring is the aerobic energy exchange expressed in kcal or J per unit time in relation to weight or patient’s body surface area (e.g. $\text{kcal} \cdot \text{m}^{-2} \cdot \text{min}^{-1}$).

However, even in the early days of the use of metabolimeters with analog hardware components, clinical physicians noticed that the instrument may be used as a current stress level indicator — patient’s functional adaptation mechanism stress. This possibility can be provided in the great majority of cases by energy-dependent, functional nature of acute adaptation, while chronic adaptation more often is provided by more energy-saving morphological method requiring, however, significant time. In due time, we have also used already new-generation digital metabolimeter for such purpose, e.g. as a monitor of adequate anesthetic protection against surgical attack [35], however, we have quickly noticed another capability. We will explain this using a clinical example.

The display screen photos of patient R. aged 52 undergoing off-pump coronary artery bypass surgery in the first hours after the operation show that with the increase in the end-expiratory pressure PEEP from 5 to 8 mbar against stable state of both parameters, curves VO_2 and VCO_2 make a synchronous „climb“ (Figure 7, a, left-hand and then right-hand curve field), but with further increase in PEEP from 8 to 11 mbar, synchronous short-term drop of both parameters is also observed; and the change in inspiratory oxygen concentration is followed by mismatched curve behavior (Figure 7, b, right-hand and left-hand fields, respectively). To explain these phenomena, we need to go back to the physiological concepts described above.

By increasing PEEP (P_{EEP}), we always increase the number of recruited alveoli all other things being equal. In our case, increase in PEEP from 5 to 8 mbar at time stamp 15:42 is followed by short-term growth of VO_2 and VCO_2 that indicates the presence of efficient perfusion in the additionally recruited alveoli, i.e. an increase of the effective pulmonary diffusion membrane area. Why is the growth of VO_2 and VCO_2 short-term in this case? The reason is that our PEEP manipulations in no case can influence the oxygen consumption level and carbon dioxide production by the body tissues, these values remain constant — and, thus, VO_2 and VCO_2 shall finally remain unchanged in the lungs. Dependence of oxygen consumption by the body tissues on systemic oxygen delivery DO_2 is known to become visible only at very low delivery levels — usually below approx. $200\text{--}250 \text{ ml} \cdot \text{m}^{-2} \cdot \text{min}^{-1}$ or $6\text{--}7 \text{ ml} \cdot \text{kg}^{-1} \cdot \text{min}^{-1}$ (Figure 8, [36]). We can see

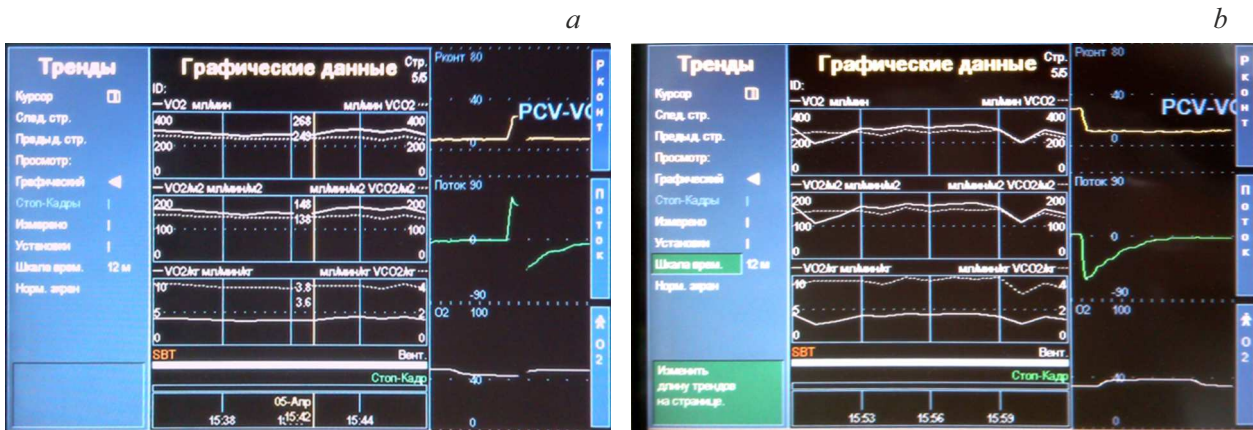


Figure 7. *a* — VO_2 (solid white lines) and VCO_2 (dashed white lines) dynamics displayed on Engström Carestation (GE Healthcare, USA) ventilator screen: in „Graphical data“ field, the upper pair of curves expressed in $ml \cdot min^{-1}$, central — $ml \cdot min^{-1} \cdot m^{-2}$, lower — $ml \cdot min^{-1} \cdot kg^{-1}$. The right-hand part of the curves shows synchronous short-term rises of VO_2 (with larger amplitude) and VCO_2 (with smaller amplitude) in response to increase in PEEP from 5 to 8 mbar *b* — the right-hand part of the trend screen shows synchronous dynamics in the form of short-term drop of both parameters after increase in PEEP from 8 to 11 mbar, the left-hand part shows VO_2 calculation artefact as a result of reduced inspiratory concentration of O_2 from 50% to 40% against permanent VCO_2 level.

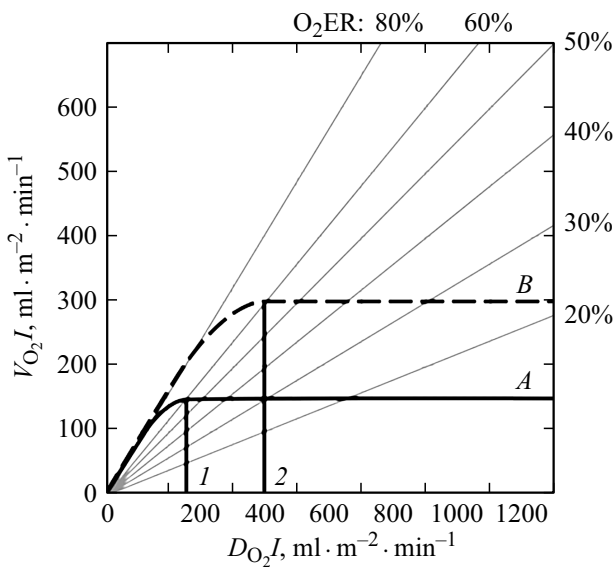


Figure 8. Systemic oxygen delivery index DO_2I (specified value is $420-720 ml \cdot m^{-2} \cdot min^{-1}$) vs. systemic oxygen consumption by the body VO_2I (specified value is $110-175 ml \cdot m^{-2} \cdot min^{-1}$) at normal (*a*) and increased (*b*) (e.g. in case of physical activity, fever, heperthyrea, etc.) aerobic energy metabolism levels. Rays outcoming from the origin of coordinates reflect various oxygen extraction levels from arterial blood O_2ER (scale on the right hand and at the bottom, normal values are 20–30%) [31].

this reset phenomenon of pulmonary VO_2 and VCO_2 on the curves: at the next stage — as soon as in some minutes! — due to increase in O_2 content and decrease in CO_2 content in the venous admixture, diffusion volume rates return to their initial values despite the increase in the diffusion membrane area. With further increase in PEEP from 8 to 11 mbar, any other alveoli pool is recruited

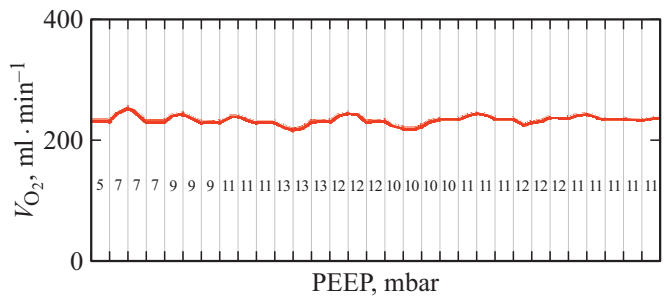


Figure 9. Diagram of optimum PEEP fitting by iteration.

additionally, however synchronous reduction of VO_2 and VCO_2 at time stamp 15:59 indicates that the respiratory surface of the lungs is reduced as a result of capillary blood flow „squeezing out“ from a part of ventilated pulmonary parenchyma. Then, however, both values return to their initial level in a couple of minutes like in the first case — regardless of the diffusion surface reduction — due to the oxygen content reduction and carbon dioxide content increase in blood flowing into the pulmonary capillaries.

Synchronous and unidirectional variation mode of VO_2 and VCO_2 is an important feature of the described dynamic phenomena. At the same time, similar variations of only one of the parameters more often reflect some or another artefacts — for example, VO_2 calculation error with change in the inspiratory oxygen concentration visible in the left half of the curves in Figure 7, *b*.

Having assured ourselves in reliable reproducibility of the described phenomena during several years, and having solved the problem of VO_2 and VCO_2 isoline stability by using the method only in the patients without unassisted breathing affected by myoplegia, we began to

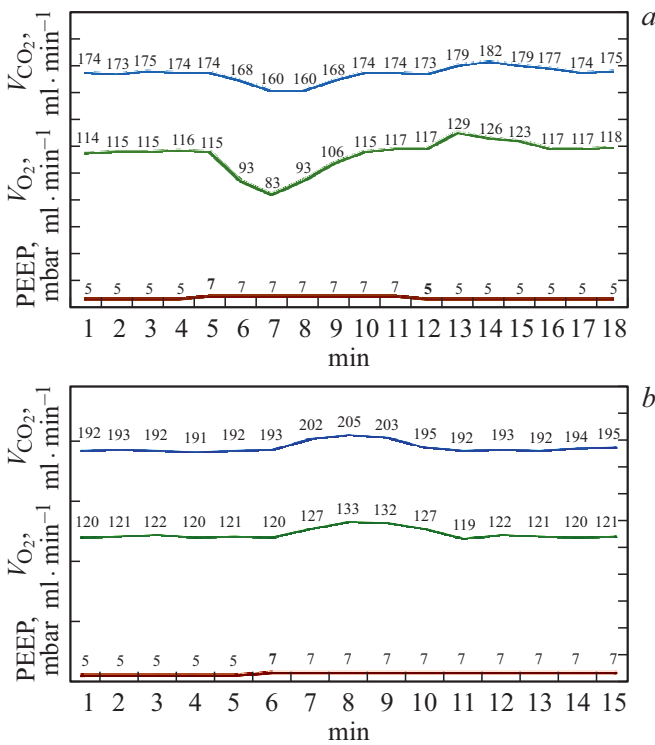


Figure 10. PEEP variations (master, at the bottom), V_{CO_2} and VO_2 (slave, at the top) during patient treatment before (a) and after (b) volume fluid management.

use metabolimeter for optimum PEEP setting in clinical conditions. Actually, this a procedure of iterative search of a PEEP boundary at which — regardless of the flow direction, from top or bottom! — synchronous „climbs“ of VO_2 and V_{CO_2} curves alternate with synchronous „pits“ (see the diagram in Figure 9). As a reference method to certify optimization of the ventilation/perfusion ratios, difference between arterial carbon dioxide stress $PaCO_2$ and end-expiratory partial pressure of carbon dioxide is calculated using capnography data P_{ETCO_2} , „ideally“ it shall be equal to zero (specified value is up to 4–5 mm Hg) [37].

The following observation is a clear example of the PEEP fitting method used in an elective cardiac surgery patient. Patient B. aged 61 had mitral valve replacement combined with on-pump RF cardiac ablation. In the next hours after the operation, a metabolographic monitor was used for PEEP level fitting in the intensive therapy unit. Initial $PaCO_2 - P_{ETCO_2}$ was equal to 1.7 mm Hg. At 15:13, increase in PEEP from 5 to 7 mbar caused the reduction of pulmonary VO_2 and V_{CO_2} which compeled to go back to 5 mbar after 8 min; this reverse maneuvre caused the rise of both curves as expected (Figure 10, a). The situation was evaluated as manifestation of relative hypovolemia (lack of bloodstream volume); volume fluid management was performed — 500 ml Gelofusin and 200 ml 10% albumin solution. After 2.5 h, at 17:47, change in PEEP from 5 to 7 mbar caused synchronous growth of VO_2 and V_{CO_2} indicating that growth of end-expiratory pressure in

these new pulmonary hemodynamics conditions does not result in blood flow squeezing out from the capillaries around the recruited alveoli (Figure 10, b). $PaCO_2 - P_{ETCO_2}$ was equal to 0.2 mm Hg at that time indicating optimization of V/Q . It is interesting that in addition to term „alveoli recruitment“ [38] widely used in intensive therapy, physiologists use term „recruitment phenomenon“ exactly as applicable to pulmonary circulation capillaries [5,6]. pulmonary circulation vascular bed is softer and the number of functioning (open, non-collapsed) pulmonary capillaries depends to a large extent on the degree of filling of this pliable volume with blood. In clinical practice, it also would be advisable to remember that alveoli recruitment is useless without adequate pulmonary capillaries recruitment!

From a practical perspective, it is very important that during the method trial process, we began to use a wide variety of commercial respiratory equipment from various manufacturers, including equipment not designed directly for metabolographic analysis. It is important that the equipment ensure real-time assessment of oxygen absorption and/or carbon dioxide release by lungs. Thus, Figure 11 shows how behavior of only one VO_2 suggests that even minimum PEEP 5 mbar may be to high in the patient with relative hypovolemia, Figure 12 shows that surrogate V_{CO_2} waves were used to set optimum PEEP, and Figure 13

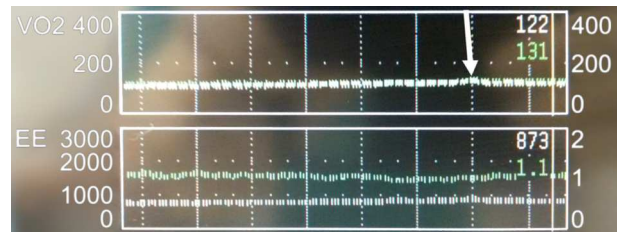


Figure 11. White arrow on VO_2 graphical trend shows a wave following the decrease in PEEP from 5 to 2 mbar using Fabius anaesthesia-respiratory apparatus (Dräger, Germany; S/5 display screen with E-CAiOVX metabolographic module, Datex Ohmeda, USA).

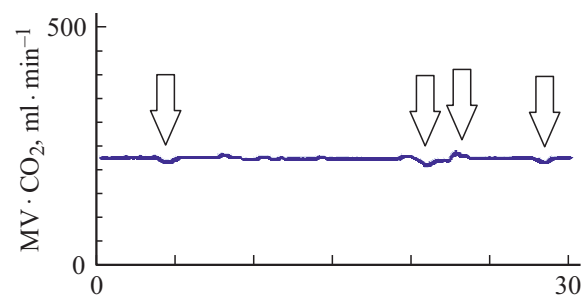


Figure 12. Waves reflecting the optimum PEEP fitting procedure are shown by white arrows on surrogate V_{CO_2} trend — products of minute breathing volume and average carbon dioxide concentration in expiratory gas mixture — reflected by respiratory monitor of Zeus anaesthesia-respiratory apparatus (Dräger, Germany). Variations with lower amplitude or duration shown in the diagram reflect the steady state line drift.

Table trend report																Printed: 20-01-2016 17:47:14	
Patient name:		Patient ID:				Patient category:				With electric cardiostimulator: Not specified							
Sex: not specified		Bed N:				Date of birth:				Height/Weight: 180 cm/74 kg							
	16-04-2021 10:30:40	16-04-2021 10:30:45	16-04-2021 10:30:50	16-04-2021 10:30:55	16-04-2021 10:31:00	16-04-2021 10:31:05	16-04-2021 10:31:10	16-04-2021 10:31:15	16-04-2021 10:31:20	16-04-2021 10:31:25	16-04-2021 10:31:30	16-04-2021 10:31:35	16-04-2021 10:31:40	16-04-2021 10:31:45	16-04-2021 10:31:50	16-04-2021 10:31:55	
Heart rate (beats/min)	59	60	61	61	60	59	60	62	62	61	60	60	61	62	62	62	
Resp. rate (br/min)	12	12	12	12	12	12	12	12	12	12	10	10	10	10	12	12	
MAC	1.1 (Age 40)	1.1 (Age 40)	1.1 (Age 40)	1.1 (Age 40)	1.1 (Age 40)	1.1 (Age 40)	1.1 (Age 40)										
MVCO ₂ (ml/min)	94	92	91	94	94	94	94	94	96	89	92	95	97	102	105	109	
MVO ₂ (ml/min)	173	172	172	174	172	172	172	172	172	168	183	196	208	220	232	245	
VCO ₂ (ml)	8	8	8	8	8	8	8	8	8	1	11	11	10	13	11	12	
VO ₂ (ml)	14	14	14	14	14	14	14	14	14	11	29	28	26	26	26	26	
PEEP (mbar)	2.2	2.2	2.1	2.1	2.0	2.2	2.2	2.2	5.8	6.4	6.8	7.0	7.4	7.6	7.6	7.9	
SPO ₂ (%)	99	99	99	99	99	99	99	99	99	99	99	99	99	99	99	99	
Pulse rate (beats/min)	58	60	61	62	61	59	59	61	62	61	59	59	61	62	63	62	

Figure 13. White arrow on SV 800 (Mindray, PRC) ventilator tabular trend printout show the time of PEEP increase from 2 to 8 mbar (this parameter is underlined with black dashed line in the table); then we can see a sudden growth of VO₂ (black line in the table) and VCO₂ (white line in the table) expressed in ml by this ventilator for each respiratory cycle.

shows the ventilator tabular trend printout with discrete VO₂ and VCO₂ for each successive respiratory cycle. It should be noted that tabular presentation of VO₂ and VCO₂ dynamic rows is more useful for identification of significant waves than graphical presentation. And in all these cases, the phenomena described above are clearly visible provided that the main condition is satisfied — absence of significant spontaneous oscillations of these two variables.

Conclusion

Taking into account the undeniable importance of the maximum involvement of collapsed alveoli in ventilation, a pertinent question always arises — do these alveoli newly recruited using mechanical lung ventilation participate in gas exchange. Routine bedside monitoring methods used for MV patients not always are able to give a clear answer, but modern clinical infrastructure still allow to change the focus of researchers', physicians' and respiratory equipment engineers' attention from maximum possible alveoli recruitment to creation of maximum effective respiratory gas diffusion surface.

Analysis of oxygen absorption and carbon dioxide elimination trends in the human respiratory cycle makes it possible not only to clearly document the mutual competition of gas and blood flows in confined pulmonary gas exchanger volume, but also to optimize the ventilation/perfusion ratios in lungs in bedside MV mode by means of positive pressure

parameter „titration“ primarily — end-expiratory pressure. It is very important that the method is not based on unique equipment of a certain manufacturer, but may be implemented using any metabolographic module which can both be integrated into anaesthesia-respiratory apparatus and be a stand-alone module.

While taking high efforts to ensure alveoli recruitment, we pay low attention to the fact that successful recruitment may be performed at cost of not only physical damage of lung tissue and systemic hemodynamics decline, but also of perfusion displacement from the lung tissue regions involved in the ventilation by means of high intra-alveolar pressure depending on the patient's volume status. As a matter of fact, mutually conjugate effects of (a) — blood flow „constriction“ in pulmonary capillaries due to high pressure in ventilated alveoli with formation of alveolar dead space, and (b) — blood flow displacement into more damaged zones with low intra-alveolar pressure and dramatic increase in intrapulmonary bypass fraction may play much more important role, than that yet recognized routinely, in the refractory hypoxemia pathophysiology. We are sure that this phenomenon requires further investigation both in terms of pathophysiology and clinical applications. From our point of view, the next logical step would be the development of an automated PEEP „titration“ tool based on detection of significant VO₂ and VCO₂ waves similar to the automatic alveoli recruitment option currently

implemented using commercial MV equipment from various manufacturers.

Conflict of interest

The authors declare that they have no conflict of interest.

References

- [1] B. Lachmann. *Intensive Care Med.*, **18**, 319 (1992). DOI: 10.1007/BF01694358
- [2] P. Van der Zee, D. Gommers. *Critical Care*, **23**, 73 (2019). DOI: 10.1186/s13054-019-2365-1
- [3] J.B. West. *Brit. Med. Bull.*, **19**, 53 (1963).
- [4] T. Des Jardin. *Cardiopulmonary Anatomy and Physiology. Essentials for Respiratory Care. 5th ed.* (Delmar, 2008), p. 628.
- [5] D.P. Droretzky, B.I. Tkachenko. *Gemodinamika v legkikh* (Meditsina, M., 1987) (in Russian)
- [6] I.S. Breslav, G.G. Isaev (otv. red.). *Fiziologiya dykhaniya. 3* (Nauka, SPb. 1994) (in Russian)
- [7] A.I. Deev. *Potoki veshchestv v rezultate diffuzii i elektrodifuzii*, v kn.: Yu.A. Vladimirov, D.I. Roshchupkin, A.Ya. Potapenko, A.I. Deev. *Biofizika* (Meditsina, M., 1983), p. 20–24 (in Russian).
- [8] W. Oczenski. *Atmen — Atemhilfen* (10 Aufl.—Stuttgart—NY., Georg Thieme Verlag, 2017), p. 580. DOI: 10.1055/b-004-140689
- [9] A.B. Lamb, R.G. Pearl. *Nunn's Applied Respiratory Physiology. 6th ed.* (Elsevier, 2005), p. 501
- [10] L.A. Sidirenko, R.S. Vinitskaya, L.L. Shik. *Byull.eksper. fisiol. i med.*, **78** (8), 13 (1974) (in Russian).
- [11] H.A. Jones, E.E. Davies, J.M. Hughes. *Bull. Eur. Physiopathol. Respir.*, **18** (2), 319 (1982).
- [12] M.P. Hlastala, F.L. Powell, J.C. Anderson. *Appl. Physiol.*, **114** (5), 675 (2013). DOI: 10.1152/jappphysiol.01291.2012
- [13] Z.L. Chen, Y.L. Song, Z.Y. Hu, S. Zhang, Y.-z. Chen. *J. Appl. Physiol.*, **119** (3), 190 (2015). DOI: 10.1152/jappphysiol.00112.2015
- [14] R.D. Hubmayr, R.H. Kallet. *Resp. Care.*, **63** (2), 219 (2018). DOI: 10.4187/respcare.05900
- [15] R.L. Riley, A.F. Cournand. *J. Appl. Physiol.*, **1** (12), 825 (1949). DOI: 10.1152/jappphysiol.1949.1.12.825
- [16] W.O. Fenn, H. Rahn, A.B. Otis. *Am. J. Physiol.*, **146**, 637 (1946).
- [17] A.S. Reynolds, A.G. Lee, J. Renz, K. DeSantis, J. Liang, C.A. Powell, C.E. Ventetuolo, H.D. Poor. *Am. J. Respir. Crit. Care Med.*, **202**, 1037 (2020). DOI: 10.1164/rccm.202006-2219LE
- [18] F. Ciceri, L. Beretta, A.M. Scandroglio, S. Colombo, G. Landoni, A. Ruggeri, J. Peccatori, A. D'Angelo, F. De Cobelli, P. Rovere-Querini, M. Tresoldi, L. Dagna, A. Zangrillo. *Crit. Care Resusc.*, **22**, 95 (2020).
- [19] U.S. Von Euler, G. Liljestrand. *Acta Physiol. Scand.*, **12** (4), 301 (1946).
- [20] J.W. Severinghaus, E.W. Swenson, T.N. Finley, M.T. Lategola, J. Williams. *J. Appl. Physiol.*, **16**, 53 (1961). DOI: 10.1152/jappphysiol.1961.16.1.53
- [21] Hrsg. von W. Siegenthaler, H.E. Blum. *Klinische Pathophysiologie* (9 Aufl.—Stuttgart—NY., Georg Thieme Verlag, 2006), p. 1178. DOI: 10.1055/b-004-134448
- [22] A.P. Zilber. *Regionarnyye funktsii legkikh* (Petrozavodsk, Karelia, 1971) (in Russian)
- [23] J.M.B. Hughes, J.B. Glazier, J.E. Maloney, J.B. West. *Respir. Physiol.*, **4**, 58 (1968). DOI: 10.1016/0034-5687(68)90007-8
- [24] M.J. Tobin. *Principles and Practice of Mechanical Ventilation. 2nd ed.* (McGraw-Hill, 2006), DOI: 10.1097/01.shk.0000245023.16612.dd
- [25] D.W. Chang. *Respiratory care Calculations. 2nd ed.* (Delmar, 1999)
- [26] K.M. Lebedinsky, V.A. Mazurok, A.V. Nefedov. *Osnovy respiratornoy podderzhki* (Tchelovek, SPb., 2007) (in Russian)
- [27] I.A. Shurygin. *Iskusstvennaya ventilatsiya legkikh kak meditsinskaya tekhnologiya* (Izdat. dom Binom, M., 2020) (in Russian)
- [28] B.D. Summ. *Osnovy kolloidnoy khimii* (Akademia, M., 2006) (in Russian)
- [29] K.M. Lebedinskii, D.A. Artyukov, M.Y. Borisov, T.A. Gromova, O.A. Slivin. *Russ. J. Anaesthesiology and Reanimatology*, **59** (4), 72 (2014).
- [30] ARDSNet Protocol. Available at: http://www.ardsnet.org/files/ventilator_protocol_2008-07.pdf (checked on 04.02.2022)
- [31] K.M. Lebedinsky (red.). *Krovoobrashcheniye i anesteziya. Otsenka i korrektsiya sistemnoy gemodinamiki vo vremia operatsii i anestezii* (Tchelovek, SPb., 2015), 2-c izd. (in Russian)
- [32] I.N. Leyderman, A.I. Gritsan, I.B. Zabolotskikh, K.Yu. Krilov, K.M. Lebedinskii, V.A. Mazurok, E.M. Nikolaenko, A.I. Yaroshetsky. *Russ. J. Anaesthesiology and Reanimatology*, **64** (4), 5 (2019). DOI: 10.17116/anaesthesiology20190415
- [33] G.C. White. *Equipment Theory for Respiratory Care. 4th ed.* (Delmar, 2005)
- [34] J.M. Cairo, S.P. Pilbeam. *Mosby's Respiratory Care Equipment. 8th ed.* (Mosby Elsevier, 2010)
- [35] A.V. Perfilova, T.A. Gromova, K.M. Lebedinskii, A.M. Zaichik. *Russ. J. Anaesthesiology and Reanimatology*, **59** (1), 43 (2014).
- [36] P.T. Schumacker, R.W. Samsel. *Crit. Care Clin.*, **5**, 255 (1989).
- [37] I.A. Shurygin. *Monitoring dykhaniya v anesteziologii i intensivnoy terapii* (Nevsky Dialekt, SPb., 2003)
- [38] A.I. Gritzan, A.I. Yaroshetzkii, A.V. Vlasenko, S.V. Gavrilin, B.R. Gelfand, I.B. Zabolotskikh, A.A. Eremenko, A.P. Zil'ber, V.L. Kassil', M.Yu. Kirov, A.P. Kolesnichenko, K.M. Lebedinskii, I.N. Leyderman, V.A. Mazurok, V.V. Moroz, M.I. Neimark, E.M. Nikolaenko, D.N. Protzenko, V.A. Rudnov, D.V. Sadchikov, M.A. Sadritdinov, A.A. Solodov, K.N. Khrapov, S.V. Tzarenko. *Russ. J. Anaesthesiology and Reanimatology*, **61** (1), 62 (2016). DOI 10.18821/0201-7563-2016-61-1-62-70